Performance Analysis of a Hybrid QAM-MPPM Technique Over Turbulence-Free and Gamma–Gamma Free-Space Optical Channels

Haitham S. Khallaf, Hossam M. H. Shalaby, José M. Garrido-Balsells, and Seiichi Sampei

***Abstract*—The performance of a hybrid *M*-ary quadrature amplitude modulation multi-pulse pulse-position modulation (hybrid QAM-MPPM) technique is investigated in both turbulence-free and gamma–gamma free-space optical (FSO) channels. Both the spectral efficiency and asymptotic power efficiency of the hybrid QAM-MPPM are estimated and compared to traditional QAM and MPPM techniques. The bit error rate (BER) of intensity-modulation direct-detection (IM-DD) systems adopting the hybrid technique is investigated over turbulence-free FSO channels. Upper-bound expressions for the average BER and outage probability are derived for FSO systems by adopting a hybrid QAM-MPPM scheme over gamma–gamma turbulent channels. In addition, the performance of a Reed–Solomon coded hybrid QAM-MPPM is considered. The obtained expressions are used to numerically investigate the performance of the hybrid technique. Our results reveal that, under the conditions of comparable data rates, the same bandwidth, and the same energy per bit, FSO systems adopting the hybrid technique outperform those adopting traditional MPPM, QAM, and on–off keying (OOK) techniques by 1.5, 0.4, and 3 dB, respectively, in the case of turbulence-free channels. Moreover, the new technique shows a better BER performance under different turbulence levels when compared with traditional MPPM and QAM techniques in turbulent FSO communication channels. Also, it shows an improvement in outage probability compared to MPPM, QAM, and OOK over gamma–gamma FSO channels.**

***Index Terms*—Atmospheric turbulence; Free- space optics; Hybrid *M*-ary quadrature amplitude modulation multi-pulse pulse-position modulation (hybrid QAM-MPPM); Gamma-gamma channels; Multi-pulse pulse-position modulation; Power efficiency; Quadrature amplitude modulation; Spectral efficiency.**

Manuscript received June 1, 2016; revised December 8, 2016; accepted December 21, 2016; published February 1, 2017 (Doc. ID 267393).

Haitham S. Khallaf is with the Department of Electronics and Communications Engineering, Egypt-Japan University of Science and Technology (E-JUST), Alexandria 21934, Egypt (e-mail: eng.h.khallaf@gmail.com).

Hossam M. H. Shalaby is with the Electrical Engineering Department, Faculty of Engineering, Alexandria University, Alexandria 21544, Egypt.

José M. Garrido-Balsells is with the Department of Communications Engineering, University of Málaga, 29071 Málaga, Spain.

Seiichi Sampei is with the Graduate School of Engineering, Osaka University, 2-1 Yamada-oka, Suita, Osaka 565-0871, Japan.

https://doi.org/10.1364/JOCN.9.000161

I. Introduction

Spectrally efficient *M*-ary quadrature amplitude modulation (QAM) is widely used in modern communication systems, where a high throughput is required under a limited bandwidth condition. It is an attractive way of increasing the spectral efficiency in optical communications. On the other hand, power-efficient multi-pulse pulse-position modulation (MPPM) has been proposed as an alternative modulation technique to standard pulse-position modulation (PPM) and on–off keying (OOK) schemes in optical communication systems [1]. The MPPM scheme presents a better bandwidth efficiency when compared to the PPM technique and a better power efficiency when compared to the OOK technique.

The idea of superimposing different modulation techniques to improve both the power and spectral efficiencies simultaneously has been proposed in many research works. Xiang *et al.* introduced a new class of optical modulation formats based on combining m-PPM or m-FSK with additional polarization and/or phase modulation [2]. Hybrid modulation based on polarization-switched quadrature phase-shift keying (PS-QPSK) and polarization-division multiplexing QPSK (PDM-QPSK) superimposed on PPM signals have been proposed in [3–5]. The proposed schemes provide higher power efficiencies than PDM-QPSK at the expense of reduced spectral efficiency. Selmy *et al.* introduced and investigated the performance of innovative hybrid modulation techniques based on combining MPPM with binary phase-shift keying (BPSK) or QPSK [6,7]. Khallaf *et al.* proposed new hybrid modulation techniques based on both orthogonal frequency-division multiplexing (OFDM)-PPM [8] and QAM-MPPM [9].

In this paper, we introduce a deeper performance analysis of the power-efficient hybrid QAM-MPPM modulation scheme introduced in [9]. In [9], the performance of optical fiber communication systems adopting the new scheme was investigated. However, in this paper, we consider the performance of free-space optical (FSO) systems adopting a hybrid QAM-MPPM scheme. A real scenario is evaluated by considering both turbulence and different noise sources, e.g., shot noise, thermal noise, and relative intensity noise. New upper-bound expressions for the average

BER and outage probability of systems adopting the hybrid scheme have been derived for gamma–gamma turbulent FSO channels. In addition, the effects of the hybrid modulation techniques' design parameters on the system performance are investigated. Finally, the performance of a Reed–Solomon (RS) coded hybrid scheme is investigated.

The remainder of this paper is organized as follows. In Section II, a mathematical model and block diagram for both the transmitter and receiver of the hybrid system are presented. In Section III, the spectral and asymptotic power efficiencies of the hybrid QAM-MPPM scheme are estimated and compared to traditional QAM and MPPM techniques. Sections IV and V are devoted to analyzing the performance of the new scheme in both turbulence-free and turbulent FSO communication channels, respectively. Our numerical results are given in Section VI, where we make comparisons among hybrid QAM-MPPM modulation techniques and traditional MPPM, QAM, and OOK. In addition, we investigate the effect of changing the hybrid scheme's parameters on the system's average BER. Also, the effect of applying RS coding is investigated. Finally, the conclusion is given in Section VII.

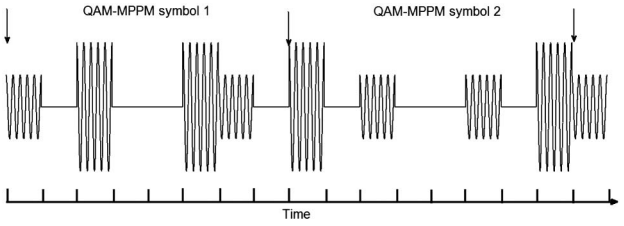

Fig. 1. Frame structure of a hybrid QAM-MPPM modulation scheme

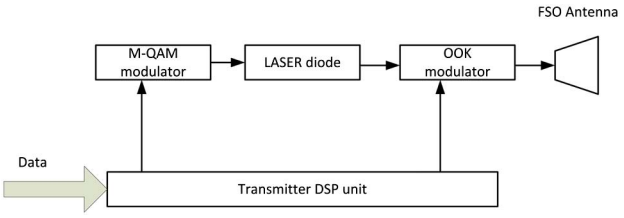

Fig. 2. Block diagram of a hybrid QAM-MPPM transmitter.

II. Hybrid QAM-MPPM System Model

In MPPM modulation techniques, the symbol duration, T, is divided into N time slots, each with duration $T_s = \frac{T}{N}$, and has optical power in w time slots only. The MPPM symbol for any number of time slots $N \geq 1$ and any $w \in \{1, 2, \ldots, N\}$ is selected from the set [10]

$$S_{\text{MPPM}} \underset{=}{\text{def}} \left\{ \mathbf{B} \in \{0,1\}^N : \sum_{i=1}^{N} B_i = w \right\}. \tag{1}$$

The cardinality of this set is $\binom{N}{w}$, and the number of bits per MPPM symbol is $\lfloor \log_2 \binom{N}{w} \rfloor$, where $\lfloor x \rfloor$ is the maximum integer less than x.

In the hybrid QAM-MPPM scheme, QAM signals are used to modulate the optical pulses within an MPPM frame, as shown in Fig. 1. The data rate, R_b, for the system adopting the hybrid QAM-MPPM technique is given in Eq. (2), where M_q is the number of QAM modulation levels,

$$R_b = \frac{\left\lfloor \log_2 \binom{N}{w} \right\rfloor + w \log_2(M_q)}{N T_s}. \tag{2}$$

The basic configurations of the transmitter and receiver for the hybrid QAM-MPPM scheme are shown in Figs. 2 and 3, respectively.

On the transmitter side, the input data are first divided into frames, each of length $w \log_2 M_q + \lfloor \log_2 \binom{N}{w} \rfloor$ bits. The first $\lfloor \log_2 \binom{N}{w} \rfloor$ bits are used to decide the locations of the w pulses, and the remaining $w \log_2 M_q$ bits are coded into w QAM symbols. Each of these symbols is signaled in one of the available w signal slots. The output optical power of the

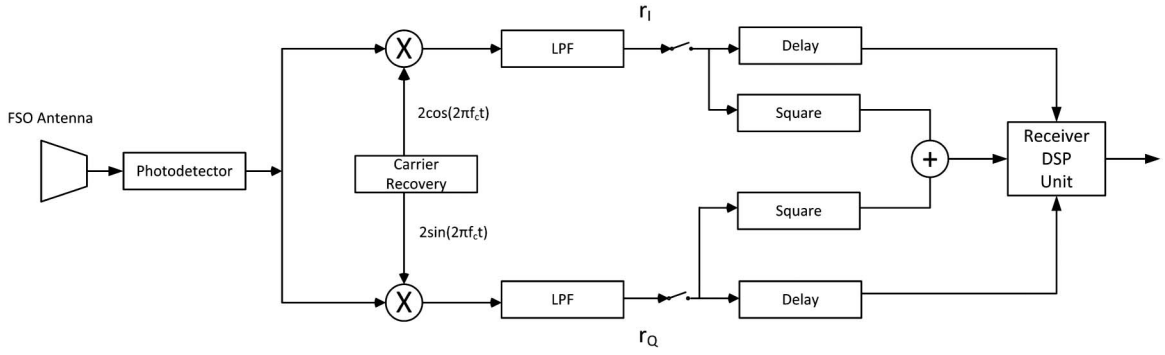

Fig. 3. Block diagram of a hybrid QAM-MPPM receiver.

OOK modulator is proportional to the modulating QAM signals as follows [11]:

$$P(t) = \frac{Np}{w}\sum_{i=0}^{N-1}[1 + MD_i(t)]B_i(t)\text{rect}\left(t - \frac{iT}{N}\right), \tag{3}$$

where p is the average transmitted optical power, M is the modulation index, and T is the duration of the hybrid symbol,

$$\begin{aligned} D_i(t) &= \begin{cases} S_{\text{QAM}}(t); & \text{for a signal time slot,} \\ 0; & \text{for a non-signal time slot,} \end{cases} \\ B_i(t) &= \begin{cases} 1; & \text{for a signal time slot,} \\ 0; & \text{for a non-signal time slot,} \end{cases} \\ \text{rect}(t) &= \begin{cases} 1; & 0 \le t < \frac{T}{N}, \\ 0; & \text{otherwise.} \end{cases} \end{aligned} \tag{4}$$

As described in the above equations, the QAM signal $S_{\text{QAM}}(t)$ is used to modulate the optical intensity of the laser diode (LD) during the signal time slots of the MPPM frame, and $S_{\text{QAM}}(t)$ is defined as [12]

$$S_{\text{QAM}}(t) = A_I\cos(2\pi f_c t) - A_Q\sin(2\pi f_c t), \qquad 0 \le t < \frac{T}{N}, \tag{5}$$

where A_I and A_Q are the signal amplitudes of the in-phase and quadrature components, respectively, and f_c is the electrical carrier frequency.

At the receiver side, the photodiode (PD) converts the received optical intensity variations into corresponding variations in the electrical domain. The output current of the PD can be written as

$$y(t) = I_{ph}\sum_{i=0}^{N-1}[1 + MD_i(t)]B_i(t)\text{rect}\left(t - \frac{iT}{N}\right) + n(t), \tag{6}$$

where $I_{ph} = \mathcal{R}\frac{Np}{w}G$ is the instantaneous photocurrent, $\mathcal{R}$ is the responsivity of the PD, $n(t)$ is Gaussian noise with variance σ_n^2, and G is the channel gain. In the case of turbulence-free FSO channels, $G = (\frac{\eta A}{\lambda L})^2$, where η is the efficiency of both the transmitter and receiver optics, λ is the operating wavelength, $A = \frac{\pi D^2}{4}$ is the transceiver telescopic area, D is the telescopic diameter, and L is the distance between the transmitter and receiver. For turbulent channels, the effects of turbulence are considered, so the channel gain is given by $G = (\frac{\eta A}{\lambda L})^2 h$, where h is the turbulent gain.

The received signal amplitudes of the in-phase and quadrature components are given by

$$r_I = MI_{ph}A_I + n_1(t), \tag{7}$$

$$r_Q = MI_{ph}A_Q + n_2(t), \tag{8}$$

respectively. Here, $n_1(t)$ and $n_2(t)$ are two Gaussian distributed random variables with zero mean and variance σ_n^2. Also, r_I and r_Q are independent Gaussian random variables with variance σ_n^2. Summation of the squares of r_I and r_Q will be used to demodulate the MPPM symbol. That is, samples of each of r_I and r_Q will be taken during each time slot, and the summation of the squares of that sample will be arranged in descending order. Then, the w largest values will refer to the location of w signal slots in the frame. After demodulating the MPPM symbol, the QAM symbol will be demodulated, and the whole symbol will be constructed. The result of the summation $X = r_I^2 + r_Q^2$ forms a new random variable that has a non-central chi-square with two degrees of freedom in the case of a signal slot and has a central chi-square with two degrees of freedom in the case of a non-signal slot. The probability density functions of X in the cases of signal and non-signal slots are given by

$$f_x(x; 2, \Omega) = \frac{1}{2}\exp\left(-\frac{x + \Omega}{2\sigma_n^2}\right)I_0\left(\frac{\sqrt{x\Omega}}{\sigma_n^2}\right), \tag{9}$$

and

$$f_x(x; 2) = \frac{1}{2}\exp\left(\frac{-x}{2\sigma_n^2}\right), \tag{10}$$

respectively, where $\Omega = (MI_{ph}A_I)^2 + (MI_{ph}A_Q)^2$, and $I_c(\cdot)$ is the cth-order modified Bessel function of the first kind. The QAM symbol desired signal power is given by [11]

$$C = \frac{1}{2}M^2 I_{ph}^2. \tag{11}$$

The signal-to-noise ratio (SNR) γ_{QAM} of the received QAM symbol is thus

$$\gamma_{\text{QAM}} = \frac{C}{\sigma_n^2}. \tag{12}$$

III. Spectral and Asymptotic Power Efficiencies of the Hybrid QAM-MPPM Scheme

In this section, we estimate both the spectral efficiency (SE) and the asymptotic power efficiency (PE) of the hybrid QAM-MPPM technique and compare it to traditional techniques in order to illustrate the motivation for the new hybrid scheme. The SE and PE of the hybrid QAM-MPPM technique are given by [10,13]

$$\begin{aligned} \text{SE} &= \frac{w\log_2 M_q + \log_2\binom{N}{w}}{N}\ \text{(bit/s)/Hz}, \\ \text{PE} &= \frac{1.5\left(w\log_2 M_q + \log_2\binom{N}{w}\right)}{w(g_l M_q - 1)}, \end{aligned} \tag{13}$$

respectively, where

$$g_l \overset{\text{def}}{=} \begin{cases} 1; & \text{if } \log_2 M_q \text{ is even,} \\ 1.25; & \text{if } \log_2 M_q \text{ is odd and } \log_2 M_q \neq 1, \\ 2; & \text{if } \log_2 M_q = 1. \end{cases} \quad (14)$$

For traditional MPPM with w signal slots and N time slots, the SE and PE are given by

$$\text{SE} = \frac{\log_2 \binom{N}{w}}{N} \text{ (bit/s)/Hz,}$$
$$\text{PE} = \frac{\log_2 \binom{N}{w}}{2w}. \quad (15)$$

For traditional QAM with M_q modulation levels, they are given by

$$\text{SE} = \log_2 M_q \text{ (bit/s)/Hz,}$$
$$\text{PE} = \frac{1.5 \log_2 M_q}{(g_l M_q - 1)}. \quad (16)$$

Figure 4 shows the SE versus 1/PE (the receiver sensitivity) for the hybrid technique (with $N = 16$, $w \in \{1, 2, \ldots, 16\}$, and $M_q \in \{4, 8, 16\}$), ordinary MPPM (with $N = 16$ and $w \in \{1, 2, \ldots, 16\}$), and ordinary QAM (with $M_q \in \{4, 8, 16\}$). It is clear from the figure that the hybrid modulation improves the receiver sensitivity when compared to ordinary QAM by {0.4, 1, 2.2} dB at SEs of {4, 3, 2} bit/sym/pol, respectively. Also, it is clear that for the same value of the PE, the hybrid technique can achieve a higher SE compared to ordinary MPPM.

In addition to the improvement in receiver sensitivity, as shown in Fig. 4, the use of the hybrid QAM-MPPM technique improves the system transmission rate in response to changes in channel status. To explain this point, we consider two communication systems: the first system adopts ordinary QAM with 8 levels, and the second system adopts the hybrid QAM-MPPM scheme with $(N, w, M_q) = (8, 4, 16)$. To cope with channel impairments, especially in the FSO channel, without increasing the average transmitted power, the first system decreases the modulation levels to 4 levels. This would decrease the transmission rate by 33.33%. For the second system, there are different choices, such as changing the system setting to $(N, w, M_q) = (8, 4, 8)$. This would decrease the transmission rate by 18%. Another solution is to change the setting to $(N, w, M_q) = (8, 3, 16)$. This would decrease the transmission rate by 22.7%. This advantage of the new technique makes it better than ordinary QAM in case they are both being used in adaptive modulation systems.

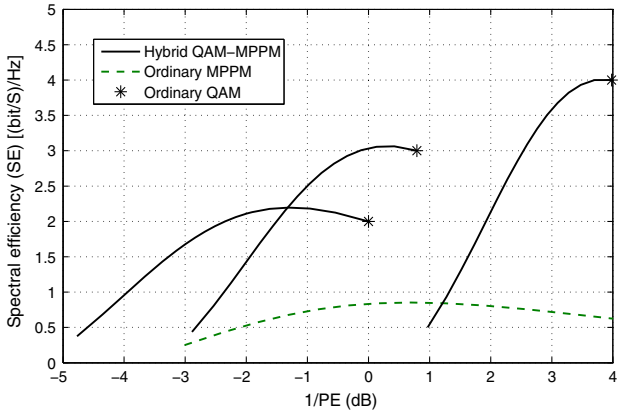

Fig. 4. Spectral efficiency versus receiver sensitivity (in dB) for both the hybrid and ordinary schemes.

IV. Performance Analysis Over Turbulence-Free FSO Channels

The BER of the hybrid QAM-MPPM scheme is the average of the BERs of both the QAM and MPPM [2]:

$$\text{BER} = \frac{\log_2 \binom{N}{w}}{\log_2 \binom{N}{w} + w \log_2 M_q} \text{BER}_{\text{MPPM}} + \frac{w \log_2 M_q}{\log_2 \binom{N}{w} + w \log_2 M_q} \times \left[(1 - \text{SER}_{\text{MPPM}}) \text{BER}_{\text{QAM}} + \frac{\text{SER}_{\text{MPPM}}}{2} \right], \quad (17)$$

where BER_{QAM} is the BER of the ordinary QAM, and SER_{MPPM} is the symbol error rate of the ordinary MPPM. The first term in Eq. (17) accounts for the BER that occurs to the group of $\lfloor \log_2 \binom{N}{w} \rfloor$ bits which is transmitted using MPPM, that is, the group has the BER of ordinary MPPM, BER_{MPPM}. The second term of the equation accounts for the BER of the remaining $w \log_2 M_q$ bits. The second term consists of two parts. The first one considers the case when the signal slot is correctly decoded, and the second considers the case of incorrect decoding. SER_{MPPM} is introduced in [14]

$$\text{SER}_{\text{MPPM}} = \sum_{l=1}^{N-w} \sum_{m=1}^{w} \int_0^{\infty} \binom{w}{m} \binom{N-w}{l} p_1 (p_{\min})^m \times (1 - P_1(p_{\min}))^{w-m} P_0(p_{\min})^{N-w-l} \times \left[(1 - P_0(p_{\min}))^l + p_0(p_{\min})^l \left(1 - \frac{1}{\binom{l+m}{m}} \right) \right] \text{d}p_{\min}, \quad (18)$$

where $p_{\min}$ denotes the minimum average power in the signal slots, $p_0(\cdot)$ and $p_1(\cdot)$ denote the average power probabilities of the non-signal and signal slots, respectively, and $P_0(\cdot)$ and $P_1(\cdot)$ denote their cumulative distributions, respectively. All these probabilities can be calculated based on the characteristics of the non-central and central chi-square distributions as given in Eqs. (9) and (10), respectively. Furthermore, the relation between BER_{MPPM} and SER_{MPPM} is given by [15]

$$\mathrm{BER}_{\mathrm{MPPM}} \le \frac{2^{\left\lfloor \log_2 \binom{N}{w} \right\rfloor - 1}}{2^{\left\lfloor \log_2 \binom{N}{w} \right\rfloor} - 1} \mathrm{SER}_{\mathrm{MPPM}}. \tag{19}$$

The BER of the ordinary Gray-coded QAM modulation technique $\mathrm{BER}_{\mathrm{QAM}}$ is given by [16]

$$\mathrm{BER}_{\mathrm{QAM}} = \begin{cases} \frac{4}{\log_2 M_q}\left(1-\frac{1}{\sqrt{M_q}}\right)\sum_{i=1}^{\sqrt{M_q}/2} \\ \quad \times Q\left((2i-1)\sqrt{\frac{3\gamma_{\mathrm{QAM}}}{M_q-1}}\right) & \text{if } k \text{ is even}, \\ \frac{4}{\log_2 M_q} Q\left(\sqrt{\frac{3\gamma_{\mathrm{QAM}}}{M_q-1}}\right) & \text{if } k \text{ is odd}, \end{cases} \tag{20}$$

where $k = \log_2 M_q$. Using Eqs. (18) and (20) in Eq. (17), we can calculate the average BER for the hybrid QAM-MPPM scheme over turbulence-free channels using numerical integration methods.

V. Performance Over Turbulent FSO Channels

The realistic channel scenario, in practice, is turbulent FSO. In this section, we investigate the performance of an FSO system by adopting the hybrid technique over turbulent channels. Atmospheric turbulence leads to random fading of the received optical irradiance, called scintillation, and causes communication degradations and link failures [17]. Both the PD current I_{ph} and the noise variance σ_n^2 are functions of channel state h, which is modeled by a gamma–gamma distribution [18],

$$f(h) = \frac{2(\alpha\beta)^{\frac{\alpha+\beta}{2}}}{\Gamma(\alpha)\Gamma(\beta)} h^{\frac{\alpha+\beta}{2}-1} K_{\alpha-\beta}\left(2\sqrt{\alpha\beta h}\right), \qquad h \ge 0, \tag{21}$$

where $\Gamma(\cdot)$ is the gamma function, $K_c(\cdot)$ is the cth-order modified Bessel function of the second kind, and α and β are scintillation parameters. In the case of plain waves, α and β are given as

$$\alpha = \left(\exp\left[\frac{0.49\sigma_R^2}{\left(1+1.11\sigma_R^{\frac{12}{5}}\right)^{\frac{7}{6}}}\right]-1\right)^{-1} \tag{22}$$

$$\beta = \left(\exp\left[\frac{0.51\sigma_R^2}{\left(1+0.69\sigma_R^{\frac{12}{5}}\right)^{\frac{5}{6}}}\right]-1\right)^{-1}. \tag{23}$$

Here, $\sigma_R^2 = 1.23 C_n^2 (2\pi/\lambda)^{\frac{7}{6}} L^{\frac{11}{6}}$ is a unitless Rytov variance, C_n^2 is the refractive-index structure parameter, L is the propagation distance, and λ is the operating wavelength. In addition, we consider the effects of different noise processes in the FSO link, which are thermal noise, shot noise, and relative intensity noise processes. The Gaussian noise models the summation of these noise processes in the FSO link [11,19], with the variance given by

$$\sigma_n^2 = \frac{\sigma_{\mathrm{th}}^2 + \sigma_{\mathrm{sh}}^2 + \sigma_{\mathrm{RIN}}^2}{T/N}, \tag{24}$$

where σ_{th}^2, σ_{sh}^2, and σ_{RIN}^2 are thermal, shot, and relative intensity noise spectral densities [A^2/Hz], respectively. $\sigma_{\mathrm{th}}^2 = \frac{4K_b T_{\mathrm{abs}} F}{R_L}$, where K_b is the Boltzmann's constant, T_{abs} is the absolute temperature, F is the noise figure of the receiver electronics, and R_L is the PD load resistor. $\sigma_{\mathrm{sh}}^2 = 2qI_{ph}$, where q is the electron charge. $\sigma_{\mathrm{RIN}}^2 = (\mathrm{RIN})I_{ph}^2$. σ_n^2 is a second-order polynomial with scintillation h as the variable.

A. BER Analysis

In order to get the average BER of the FSO system, we have to calculate the average of both $\mathrm{BER}_{\mathrm{MPPM}}$ and $\mathrm{BER}_{\mathrm{QAM}}$ over $f(h)$. For simplicity, we approximate the summations of the squares of r_I and r_Q by Gaussian random variables [20]. The SER of the MPPM is given by [14]

$$\mathrm{SER}_{\mathrm{MPPM}}(h) \le \frac{\binom{N}{w}-1}{2} \mathrm{erfc}\left(\frac{\mathcal{R}p\left(\frac{\eta A}{\lambda L}\right)^2 h}{2w}\sqrt{\frac{N}{\langle\sigma_n^2\rangle}\log_2\binom{N}{w}}\right), \tag{25}$$

where $\langle\sigma_n^2\rangle$ is the mean of the noise variance with respect to the channel state h, which is given as follows:

$$\langle\sigma_n^2\rangle = \frac{4K_b T_{\mathrm{abs}} F}{R_L(T/N)} + 2q\mathcal{R}\frac{N^2 p}{wT} + \mathrm{RIN}\left(\mathcal{R}\frac{N}{w}p\right)^2 \frac{\Gamma(\alpha+2)\Gamma(\beta+2)N}{\Gamma(\alpha)\Gamma(\beta)(\alpha\beta)^2 T}. \tag{26}$$

In order to get closed-form upper-bound expressions for $\mathrm{SER}_{\mathrm{MPPM}}$ and $\mathrm{BER}_{\mathrm{QAM}}$, we average σ_n^2 independently over the gamma–gamma channels, as given in Eq. (26), then use this value as channel independent when we derive the upper-bound expressions [11]. The average of $\mathrm{SER}_{\mathrm{MPPM}}(h)$ is evaluated in [14], as given in Eq. (27). $G_{p,q}^{a,b}(\cdot|\cdot)$ is the Meijer G-function defined in [21, Eq. (07.34.02.0001.01)], and

$$\mathrm{SER}_{\mathrm{MPPM}} \le \frac{\left(\binom{N}{w}-1\right)(2)^{\alpha+\beta-3}}{\pi^{3/2}\Gamma(\alpha)\Gamma(\beta)} \cdot G_{5,2}^{2,4}\left(\left\{\frac{4\left(\mathcal{R}p\left(\frac{\eta A}{\lambda L}\right)^2\right)^2 N\log_2\binom{N}{w}}{w^2\langle\sigma_n^2\rangle\alpha^2\beta^2}\right\} \middle| \begin{matrix} \frac{1-\beta}{2}, \frac{2-\beta}{2}, \frac{1-\alpha}{2}, \frac{2-\alpha}{2}, 1 \\ 0, 0.5 \end{matrix}\right). \tag{27}$$

To get the average of $\mathrm{BER}_{\mathrm{QAM}}(h)$, the $Q(\cdot)$ function in Eq. (20) is expressed in terms of the Meijer G-function [21, Eq. (07.34.03.0619.01)]:

$$Q(x) = \frac{1}{2\sqrt{\pi}} G_{1,2}^{2,0}\left(\frac{x^2}{2}\middle| \begin{matrix} 1 \\ 0, 0.5 \end{matrix}\right). \tag{28}$$

Based on the general integration formula in [21, Eq. (07.34.21.0013.01)], the average BER for the QAM modulation technique over turbulent channels is as given in Eq. (29). By substituting Eqs. (27) and (29) into Eq. (17), we get an upper-bound expression for the BER of the FSO system adopting hybrid QAM-MPPM over gamma–gamma turbulent channels:

$$\mathrm{BER}_{\mathrm{QAM}} = \begin{cases} \frac{(2)^{\alpha+\beta-1}\left(1-\frac{1}{\sqrt{M_q}}\right)}{\pi^{3/2}\Gamma(\alpha)\Gamma(\beta)\log_2(M_q)} \sum_{i=1}^{\sqrt{(M_q)}/2} G_{5,2}^{2,4}\left(\left\{\frac{6(2i-1)^2\left(\mathcal{R}\frac{MNp}{w}\left(\frac{\eta A}{\lambda L}\right)^2\right)^2}{\langle\sigma_n^2\rangle(M_q-1)(\alpha\beta)^2}\right\}\middle| \begin{matrix} \frac{1-\beta}{2}, \frac{2-\beta}{2}, \frac{1-\alpha}{2}, \frac{2-\alpha}{2}, 1 \\ 0, 0.5 \end{matrix}\right); & \text{if } k \text{ is even,} \\ \frac{(2)^{\alpha+\beta-1}}{\pi^{3/2}\Gamma(\alpha)\Gamma(\beta)\log_2(M_q)} G_{5,2}^{2,4}\left(\left\{\frac{6\left(\mathcal{R}\frac{MNp}{w}\left(\frac{\eta A}{\lambda L}\right)^2\right)^2}{\langle\sigma_n^2\rangle(M_q-1)(\alpha\beta)^2}\right\}\middle| \begin{matrix} \frac{1-\beta}{2}, \frac{2-\beta}{2}, \frac{1-\alpha}{2}, \frac{2-\alpha}{2}, 1 \\ 0, 0.5 \end{matrix}\right); & \text{if } k \text{ is odd.} \end{cases} \tag{29}$$

B. Outage Probability Analysis

Another metric for quantifying the performance of FSO communication systems over fading channels is the outage probability P_{out}. It is the probability that the BER of the system is higher than a threshold error rate. Also, it is defined as the probability that the instantaneous SNR γ falls below a specified threshold γ_{th}, where γ_{th} is the value of the SNR corresponding to the BER threshold $\mathrm{BER}_{\mathrm{th}}$ [11],

$$P_{\mathrm{out}} = pr(\mathrm{BER} \geq \mathrm{BER}_{\mathrm{th}}) = pr(\gamma \leq \gamma_{\mathrm{th}}). \tag{30}$$

The BER of the hybrid scheme is the average of the BERs of both the ordinary MPPM and QAM. Therefore, if we substitute the BER of each of them with the threshold value $\mathrm{BER}_{\mathrm{th}}$ in Eq. (17), the net BER will be of the same order of $\mathrm{BER}_{\mathrm{th}}$. In other words, we can write an upper bound for the outage probability of FSO systems by adopting the hybrid QAM-MPPM scheme as follows:

$$P_{\mathrm{out}} \leq 1 - \left(1 - P_{\mathrm{out}}^{\mathrm{MPPM}}\right)\left(1 - P_{\mathrm{out}}^{\mathrm{QAM}}\right), \tag{31}$$

where $P_{\mathrm{out}}^{\mathrm{MPPM}}$ and $P_{\mathrm{out}}^{\mathrm{QAM}}$ are the outage probabilities of the ordinary MPPM and the ordinary QAM, respectively. γ_{th} can be evaluated based on $\mathrm{BER}_{\mathrm{th}}$ for both the MPPM and QAM schemes from Eqs. (25) and (20), respectively, as follows:

$$\gamma_{\mathrm{th}}^{\mathrm{MPPM}} = \frac{4w^2}{N\log_2\binom{N}{w}}\left(\mathrm{erfc}^{-1}\left[\frac{\left(2^{\log_2\binom{N}{w}}-1\right)\mathrm{BER}_{\mathrm{th}}}{2^{\log_2\binom{N}{w}-2}\left(\binom{N}{w}-1\right)}\right]\right)^2, \tag{32}$$

$$\gamma_{\mathrm{th}}^{\mathrm{QAM}} = \frac{4(M_q-1)}{3M^2}\left(\mathrm{erfc}^{-1}\left[\frac{\mathrm{BER}_{\mathrm{th}}\log_2(M_q)}{2}\right]\right)^2. \tag{33}$$

Let h_{th} be the channel state corresponding to the threshold SNR γ_{th}, which is given for each of the ordinary schemes as follows:

$$h_{\mathrm{th}}^{\mathrm{MPPM}} = \frac{\sqrt{\gamma_{\mathrm{th}}^{\mathrm{MPPM}}\langle\sigma_n^2\rangle}}{\mathcal{R}p\left(\frac{\eta A}{\lambda L}\right)^2}, \tag{34}$$

$$h_{\mathrm{th}}^{\mathrm{QAM}} = \frac{\sqrt{2\gamma_{\mathrm{th}}^{\mathrm{QAM}}\langle\sigma_n^2\rangle}}{M\mathcal{R}p\frac{N}{w}\left(\frac{\eta A}{\lambda L}\right)^2}. \tag{35}$$

By substituting for the Bessel function in Eq. (21) using the Meijer G-function, where $K_v(\sqrt{z}) = \frac{1}{2}G_{0,2}^{2,0}\left(\frac{z}{4}\middle| \begin{matrix} -, - \\ \frac{v}{2}, \frac{-v}{2} \end{matrix}\right)$ [21, Eq. (03.04.26.0006.01)], the outage probability for a given γ_{th} can be written as follows:

$$P_{\mathrm{out}}(\gamma_{\mathrm{th}}) = \int_0^{h_{\mathrm{th}}} \frac{(\alpha\beta)^{\frac{\alpha+\beta}{2}}}{\Gamma(\alpha)\Gamma(\beta)} h^{\frac{\alpha+\beta}{2}-1} G_{0,2}^{2,0}\left(\alpha\beta h\middle| \begin{matrix} -, - \\ \frac{\alpha-\beta}{2}, \frac{\beta-\alpha}{2} \end{matrix}\right) \mathrm{d}h. \tag{36}$$

Using the integration formula given in [21, Eq. (07.34.21.0003.01)], the average outage probability can be written as follows:

$$P_{\mathrm{out}}(\gamma_{\mathrm{th}}) = \frac{(\alpha\beta)^{\frac{\alpha+\beta}{2}}}{\Gamma(\alpha)\Gamma(\beta)} h_{\mathrm{th}}^{\frac{\alpha+\beta}{2}-1} G_{1,3}^{2,1}\left(\alpha\beta h_{\mathrm{th}}\middle| \begin{matrix} 1-\frac{\alpha+\beta}{2} \\ \frac{\alpha-\beta}{2}, \frac{\beta-\alpha}{2}, -\frac{\alpha+\beta}{2} \end{matrix}\right). \tag{37}$$

Using Eqs. (34), (35), and (37), both $P_{\mathrm{out}}^{\mathrm{MPPM}}$ and $P_{\mathrm{out}}^{\mathrm{QAM}}$ can be evaluated. By substituting them into Eq. (31), the average outage probability of the hybrid scheme can be evaluated.

C. RS Coded Hybrid QAM-MPPM Scheme

In this section, we consider the effect of forward error correction (FEC) techniques on FSO system performance under fading channels, which is generally well known to provide significant benefits over turbulence-impaired fading channels. Here, we consider RS coding to show the improvement in FSO systems when using the FEC. The hybrid QAM-MPPM is used to modulate RS codes in the transmitter, and at the receiver, the signal is demodulated and RS decoded. An RS code can be denoted by RS (a, b), where a is the codeword length, and b is the information word length. The RS(a, b) code can correct up to $t = \frac{a-b}{2}$ code symbol errors [22]. The SER for RS(a, b), $\mathrm{SER}_{\mathrm{RS}}$, is given as [22]

$$\mathrm{SER}_{\mathrm{RS}} \le \frac{1}{a} \sum_{i=t+1}^{a} i \binom{a}{i} \mathrm{SER}^i (1 - \mathrm{SER})^{a-i}, \tag{38}$$

where SER is the symbol error rate of the hybrid QAM-MPPM scheme, which is evaluated using

$$\mathrm{SER} = 1 - (1 - \mathrm{SER}_{\mathrm{MPPM}})(1 - \log_2(M_q)\mathrm{BER}_{\mathrm{QAM}})^w. \tag{39}$$

VI. Numerical Results

In this section, we investigate the BER performances of the systems adopting hybrid QAM-MPPM modulation techniques using new expressions obtained in the previous subsections for both the turbulence-free and gamma–gamma turbulent FSO channels. We compare our results to those of the equivalent systems adopting ordinary MPPM, QAM, and OOK schemes. We choose the parameters for systems so they have comparable data rates, the same average energy, the same bandwidth, and the same channel states. In addition, we analyze the effects of the number of time slots w and the cardinality of the MPPM techniques on the BER performance of FSO systems adopting the new technique over turbulent channels. Finally, the improvement in system performance due to applying RS coding has been shown. In all our evaluations below, we use the system parameters listed in Table I.

A. Turbulence-Free Communication Channels

Figure 5 shows the average BER versus the average received optical power in (dBm) for the hybrid QAM-MPPM, with modulation index $M = 0.9$, and the ordinary MPPM. It is clear that the hybrid QAM-MPPM scheme outperforms the ordinary MPPM. Specifically, the new hybrid scheme saves about 1.5 dB in average power when compared to the ordinary MPPM at a BER of 10^{-10}. The system adopting the hybrid technique transmits 2 pulses only during 12 time slots, while that adopting the ordinary MPPM transmits 5 pulses during the same number of time slots in order to have the same number of bits per symbol. That is, the system adopting the hybrid scheme has more power concentration, which is the reason for the power savings.

TABLE I
System Parameters

Parameter	Symbol	Value
Tx/Rx optics efficiency	η	0.8
Photodiode responsivity	R	0.5 A/W
Transmitter and receiver telescopic diameter	D	8 cm
Distance	L	3 km
Relative intensity noise	RIN	−130 dB/Hz
Thermal noise spectral density	σ_{th}^2	−215 dB/Hz
Time slot duration	T_s	10^{-9} s
Operating wavelength	λ	1550 nm
PD load resistor	R_L	50 Ω

Figures 6 and 7 show the average BER versus the average received optical power in (dBm) for the hybrid QAM-MPPM and both ordinary QAM and OOK, respectively. In order to keep the condition of the same data rate, bandwidth, and energy per bit, we chose the symbol duration of both ordinary QAM and OOK to be equal to the duration of the time slot in the hybrid scheme, and all three schemes have the same average power. Two system settings for the hybrid scheme are used in both Figs. 6 and 7. In Fig. 6, at a low received optical power, <−23.25 dBm, using the hybrid system with a high power concentration, $\frac{N}{w} = \frac{32}{7}$, shows a better performance when compared to that using $(N = 4, w = 2)$ because the power concentration helps in improving the SNR for both the MPPM and QAM portions of the hybrid scheme. As the power increases over those values, the effect of the MPPM constellation size, $\binom{N}{w}$, has the dominant effect on the hybrid system performance, so the performance of the hybrid system with the lower MPPM constellation size, $(N = 4, w = 2)$, outperforms both the hybrid system with the large MPPM constellation size, $(N = 32, w = 7)$, and the ordinary QAM system. At a high received optical power, >−23.25 dBm in Fig. 6, the hybrid technique outperforms that adopting the traditional QAM

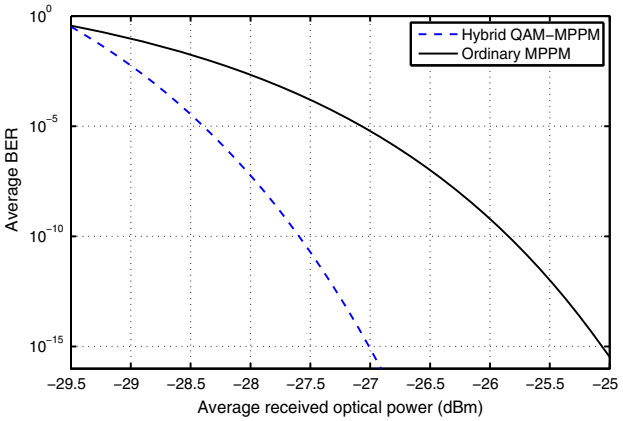

Fig. 5. Average BERs for both hybrid QAM-MPPM (with $N = 12$, $w = 2$, $M_q = 4$ and $R_b = 833$ Mbps), and ordinary MPPM (with $N = 12$, $w = 5$, and $R_b = 750$ Mbps) versus the average received optical power in dBm.

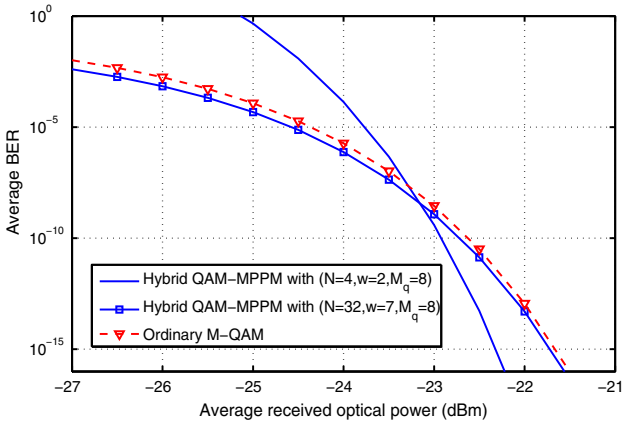

Fig. 6. Average BERs for both hybrid QAM-MPPM (with $N = 4$, $w = 2$, $M_q = 8$, and $R_b = 2$ Gbps), ($N = 32$, $w = 7$, $M_q = 8$, and $R_b = 2$ Gbps)) and ordinary QAM (with $M_q = 4$ and $R_b = 2$ Gbps) versus the average received optical power in dBm.

technique by 0.4 dB at BER $= 10^{-10}$. In order to outperform the ordinary QAM over all levels of received optical power, we need to use settings that cause a high power concentration in the low received optical power region, and in the high received optical power region, we should choose settings with a low MPPM constellation size. In Fig. 7, we can see that using more power concentration improves the system performance over all regions of received optical power. The hybrid scheme, with the setting $(N = 32, w = 5, M_q = 8)$, outperforms the OOK scheme over all levels of received optical power. The hybrid scheme using $(N = 4, w = 1, M_q = 4)$ outperforms OOK in the high received optical power region, >-27 dBm.

B. Turbulent Communication Channels

1) Hybrid Scheme Versus Ordinary Schemes: Figures 8–10 show the BER performances of the hybrid QAM-MPPM scheme versus the three ordinary modulation techniques in the case of turbulent FSO channels. The performance of the systems is investigated in the cases of both moderate and strong turbulence channels, $C_n^2 = 3 \times 10^{-15}$ m$^{-2/3}$ and $C_n^2 = 7.5 \times 10^{-15}$ m$^{-2/3}$, respectively. The modulation index value is $M = 0.4$. It is clear that the performance of the system adopting the hybrid technique outperforms the ordinary MPPM by 6 dB at a BER of 10^{-4} in the moderate turbulence channels and has a BER floor lower than that of the ordinary MPPM in strong turbulence channels. When compared to ordinary QAM, the system adopting the new technique outperforms by 2 dB at a BER of 10^{-3} in the moderate turbulence channels and by 1.5 dB at a BER of 10^{-2} in the strong turbulence channels.

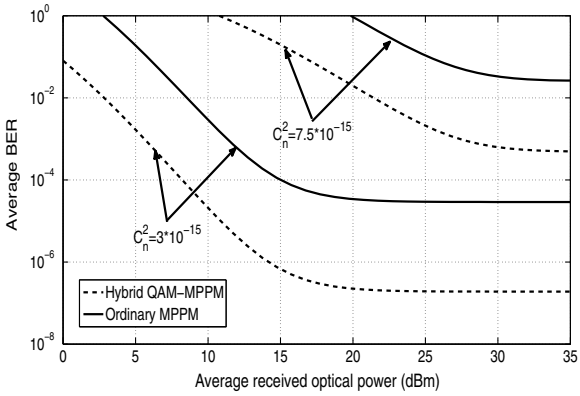

Fig. 8. Average BERs for both hybrid QAM-MPPM (with $N = 12$, $w = 2$, $M_q = 4$, and $R_b = 833$ Mbps) and ordinary MPPM (with $N = 12$, $w = 5$, and $R_b = 750$ Mbps) versus the average received optical power in dBm.

When compared to OOK, both of the modulation techniques show similar BER performances. Although both OOK and the hybrid scheme show a similar error rate under turbulence, the latter scheme has two advantages when compared to the OOK scheme. First, the hybrid scheme shows a better outage probability, as will be shown in the next paragraph. Second, the data rates in the hybrid

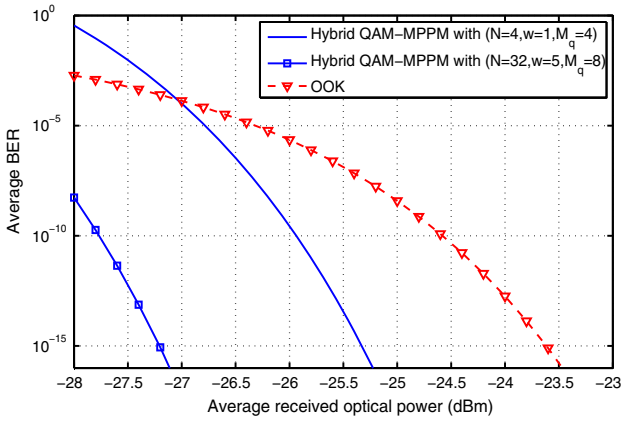

Fig. 7. Average BERs for both hybrid QAM-MPPM [with ($N = 4$, $w = 1$, and $M_q = 4$), ($N = 32$, $w = 5$, and $M_q = 8$)] and OOK, with $R_b = 1$ Gbps, versus the average received optical power in dBm.

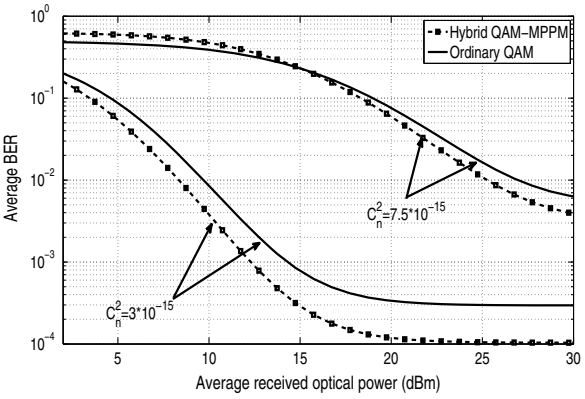

Fig. 9. Average BERs for both hybrid QAM-MPPM (with $N = 4$, $w = 2$, $M_q = 8$, and $R_b = 2$ Gbps) and ordinary QAM (with $M_q = 4$ and $R_b = 2$ Gbps) versus the average received optical power in dBm.

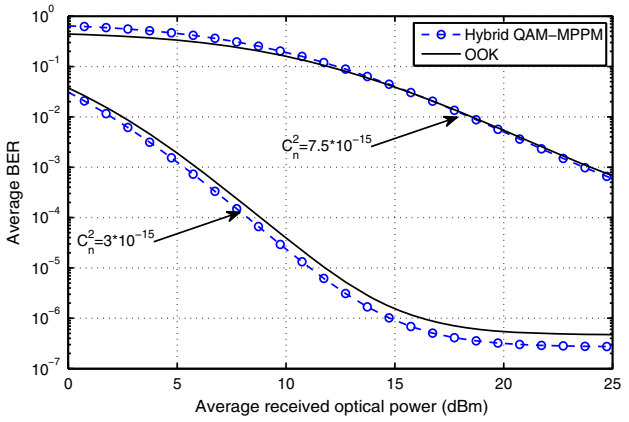

Fig. 10. Average BERs for both hybrid QAM-MPPM (with $N = 4$, $w = 1$, $M_q = 4$, and $R_b = 1$ Gbps) and OOK (with $R_b = 1$ Gbps) versus the average received optical power in dBm.

scheme can be changed by simply changing the scheme setting without changing the bandwidth of the electrical signal.

Figures 11–13 show the outage probabilities of the hybrid QAM-MPPM scheme versus the three ordinary modulation techniques over the moderate turbulence channel, $C_n^2 = 2 \times 10^{-15}$ m$^{-2/3}$. Two cases for BER$_{\text{th}}$ are considered, BER$_{\text{th}} \in \{10^{-3}, 10^{-9}\}$. System performances are compared at an outage probability $P_{\text{out}} = 10^{-2}$. The hybrid QAM-MPPM outperforms ordinary MPPM by 4 and 2.1 dB at BER$_{\text{th}} = 10^{-3}$ and 10^{-9}, respectively. Compared to the ordinary QAM, the hybrid scheme outperforms the ordinary one by 1 dB at BER$_{\text{th}} = 10^{-3}$, and they show the same outage probabilities at BER$_{\text{th}} = 10^{-9}$. Finally, compared to OOK, the hybrid scheme outperforms it by 2.2 and 1.8 dB at BER$_{\text{th}} = 10^{-3}$ and 10^{-9}, respectively, while OOK has lower outage floors in the two cases.

2) Investigation of Design Parameters' Effects: In this subsection, we investigate the effect of changing the setting of the hybrid technique's parameters on the BER performance of the system under moderate turbulence channels,

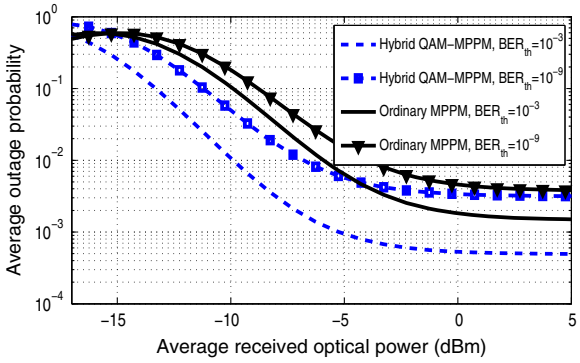

Fig. 11. Average outage probabilities for both hybrid QAM-MPPM (with $N = 32$, $w = 6$, $M_q = 4$, and $R_b = 933$ Mbps) and ordinary MPPM (with $N = 32$, $w = 16$, and $R_b = 911$ Mbps) versus the average received optical power in dBm under moderate turbulence $C_n^2 = 2 * 10^{-15}$.

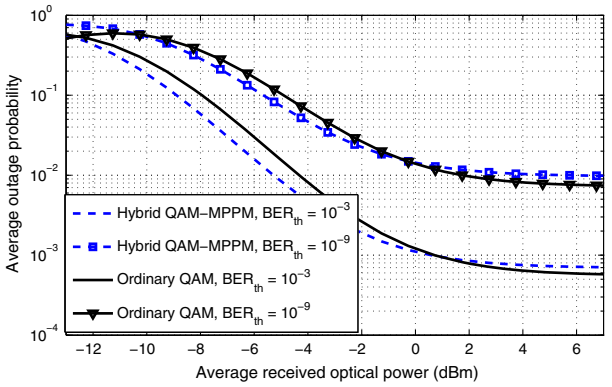

Fig. 12. Average outage probabilities for both hybrid QAM-MPPM (with $N = 4$, $w = 2$, $M_q = 8$, and $R_b = 2$ Gbps) and ordinary QAM (with $M_q = 4$ and $R_b = 2$ Gbps) versus the average received optical power in dBm under moderate turbulence $C_n^2 = 2 * 10^{-15}$.

$\sigma_r = 0.5463$, taking into consideration the different noise sources mentioned in previous sections. The modulation index value is $M = 0.4$.

First, we investigate the effect of changing the number of signal time slots w on the BER performance. We have chosen the systems' settings so that the conditions of the same bandwidth, comparable data rate, and same energy per bit are met. Although decreasing w for fixed N would increase the average received power during the signal slots, which means increasing the average power available for the QAM symbols, the number of QAM modulation levels M_q must increase in order to meet the constraint of comparable data rates. Decreasing w will improve the performance of the MPPM system, while increasing M_q and the received power at the same time may or may not improve the performance of the QAM technique.

Figure 14 shows that meaning, the performance of the system with the setting $(N, w, M_q) = (32, 9, 16)$ outperforms that using the setting $(N, w, M_q) = (32, 6, 128)$. Although the first one has a higher number of time slots, it uses a

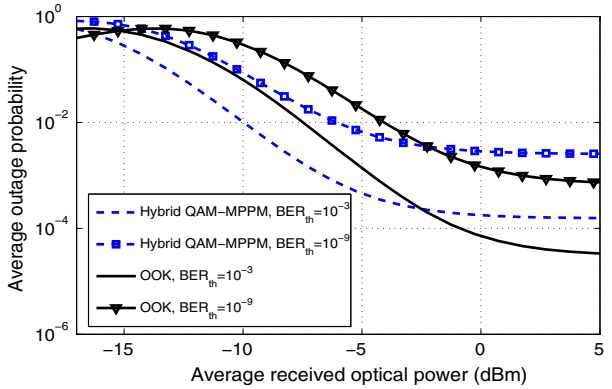

Fig. 13. Average outage probabilities for both hybrid QAM-MPPM (with $N = 4$, $w = 1$, $M_q = 4$, and $R_b = 1$ Gbps) and OOK with $R_b = 2$ versus the average received optical power in dBm under moderate turbulence $C_n^2 = 2 * 10^{-15}$.

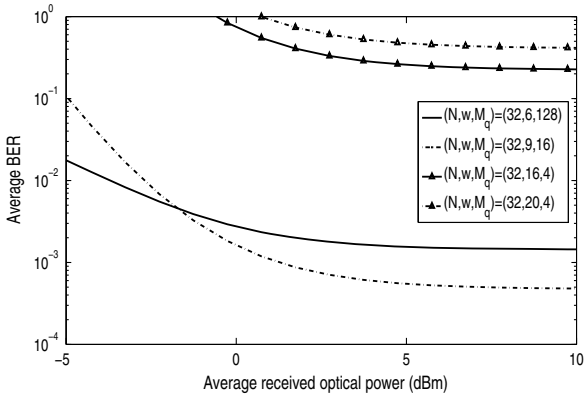

Fig. 14. Average BERs versus average received optical power in dBm for hybrid QAM-MPPM with different values of w: $((N, w, M_q, R_b) = [(32, 6, 128, 1.9$ Gbps), (32, 9, 16, 1.87 Gbps), (32, 16, 4, 1.9 Gbps), (32, 20, 4, 2 Gbps)].

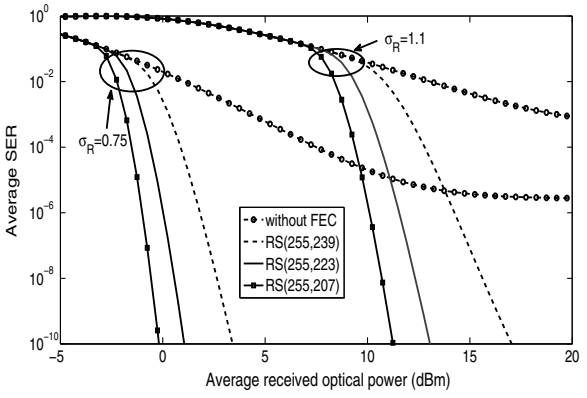

Fig. 16. Average symbol error rates versus average received optical power in dBm for hybrid QAM-MPPM with $(N, w, M_q, R_b) = (4, 2, 8, 430$ Mbps) for different RS code settings over moderate and strong turbulence channels.

lower number of QAM modulation levels. Each of these systems has a BER that is better than the two systems with $(N, w, M_q) = (32, 16, 4)$ and (32, 20, 4), although the second group has a lower number of QAM modulation levels.

Figure 15 shows the effect of the cardinality of the constellation of MPPM on the net BER of the new scheme. As shown in the figure, the higher the cardinality, the lower the system performance. As the number of symbols $\binom{N}{w}$ increases, the SER of MPPM would increase, as given in Eq. (27), and the net BER of the hybrid modulation technique would increase as well.

3) RS-Coded Hybrid QAM-MPPM: Figure 16 shows the performance of the RS-coded hybrid QAM-MPPM scheme, with $(N, w, M_q, R_b) = (4, 2, 8, 430$ Mbps), over strong and moderate turbulence channels, $\sigma_R = 1.1$ and $\sigma_R = 0.75$, respectively, with different RS code settings. RS(255, 239), RS(255, 223), and RS(255, 207) are investigated. These RS codes can correct up to 8, 16, and 24 symbol errors, respectively, with each symbol 8 bits in length. As shown in Fig. 16, the use of RS channel coding provides a significant improvement over the turbulence channel. The coded scheme outperforms that without coding by more than 7.5 dB at SER $= 10^{-3}$ in the case of a strong turbulence channel and by more than 10 dB at SER $= 10^{-5}$ in the case of a moderate turbulence channel. It is noted that using the RS(255, 223) and RS(255, 207) codes improves the system performance by 2 and 3 dB, respectively, when compared with that of RS(255, 239).

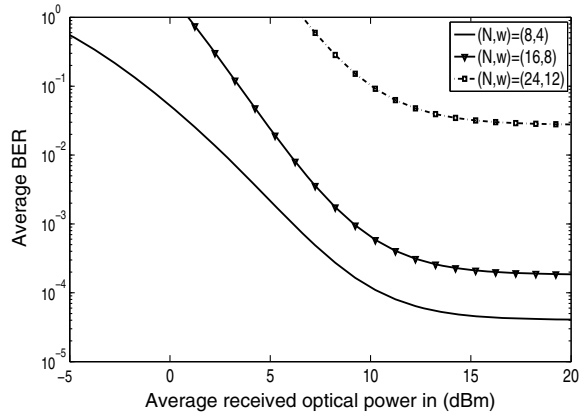

Fig. 15. Average BERs versus average received optical power in dBm for hybrid QAM-MPPM with different settings: $(N, w, R_b) = [(8, 4, 2.25$ Gbps), (16, 8, 2.3 Gbps), (24, 12, 2.37 Gbps)].

VII. Conclusion

The performance of a hybrid QAM-MPPM modulation technique has been investigated. The block diagrams for both the transmitter and receiver for the new technique have been introduced. The BER performances of the hybrid scheme for both turbulence-free and gamma–gamma turbulent FSO channels have been investigated. The BER performance of the hybrid QAM-MPPM scheme has been compared to those of traditional QAM, MPPM, and OOK schemes under the conditions of a comparable transmitted data rate, the same bandwidth, the same average energy, and the same channel state. Our results reveal that the system adopting the hybrid scheme outperforms systems adopting traditional techniques and is more power efficient. The effect of the number of signal slots w and the cardinality of the MPPM symbols on the BER of FSO systems adopting the new technique are investigated as well.

References

[1] H. Sugiyama and K. Nosu, "MPPM: A method for improving the band utilization efficiency in optical PPM," *J. Lightwave Technol.*, vol. 7, no. 3, pp. 465–472, Mar. 1989.

[2] X. Liu, S. Chandrasekhar, T. H. Wood, R. W. Tkach, P. J. Winzer, E. C. Burrows, and A. R. Chraplyvy, "M-ary pulse-position modulation and frequency-shift keying with additional polarization/phase modulation for high-sensitivity optical

transmission," *Opt. Express*, vol. 19, no. 26, pp. B868–B881, 2011.

[3] E. Agrell and M. Karlsson, "Power-efficient modulation formats in coherent transmission systems," *J. Lightwave Technol.*, vol. 27, no. 22, pp. 5115–5126, 2009.

[4] M. Karlsson and E. Agrell, "Generalized pulse-position modulation for optical power-efficient communication," in *37th European Conf. and Exhibition on Optical Communication (ECOC)*, 2001.

[5] X. Liu, T. H. Wood, R. W. Tkach, and S. Chandrasekhar, "Demonstration of record sensitivity in an optically pre-amplified receiver by combining PDM-QPSK and M-ary pulse-position modulation," *J. Lightwave Technol.*, vol. 30, no. 4, pp. 406–413, 2012.

[6] H. Selmy, H. M. H. Shalaby, and Z. Kawasaki, "Proposal and performance evaluation of a hybrid BPSK-modified MPPM technique for optical fiber communications systems," *J. Lightwave Technol.*, vol. 31, no. 22, pp. 3535–3545, 2013.

[7] H. Selmy, H. M. Shalaby, and Z. Kawasaki, "Enhancing optical multipulse pulse position modulation using hybrid QPSK-modified MPPM," in *Proc. IEEE Photonics Conf. (IPC)*, San Diego, CA, Oct. 2014, pp. 617–618.

[8] H. S. Khallaf, H. M. H. Shalaby, and Z. Kawasaki, "Proposal of a hybrid OFDM-PPM technique for free space optical communications systems," in *Proc. IEEE Photonics Conf. (IPC)*, Bellevue, WA, Sept. 2013, pp. 287–288.

[9] H. S. Khallaf and H. M. H. Shalaby, "Proposal of a hybrid QAM-MPPM technique for optical communications systems," in *Proc. 16th Int. Conf. on Transparent Opticical Networks (ICTON)*, Graz, Austria, 2014, paper Tu.B1.7.

[10] H. M. H. Shalaby, "Maximum achievable constrained power efficiencies of MPPM-LQAM techniques," *IEEE Photon. Technol. Lett.*, vol. 27, no. 12, pp. 1265–1268, 2015.

[11] A. Bekkali, C. B. Naila, K. Kazaura, K. Wakamori, and M. Matsumoto, "Transmission analysis of OFDM-based wireless services over turbulent radio-on-FSO links modeled by gamma–gamma distribution," *IEEE Photon. J.*, vol. 2, no. 3, pp. 510–520, 2010.

[12] K. Cho, D. Yoon, W. Jeong, and M. Kavehrad, "BER analysis of arbitrary rectangular QAM," in *35th Asilomar Conf. on Signals, Systems and Computers*, Pacific Grove, CA, 2001, pp. 1056–1059.

[13] S. Benedetto and E. Biglieri, *Principles of Digital Transmission: With Wireless Applications*. New York, USA: Kluwer, 1999.

[14] A. E. Morra, H. S. Khallaf, H. M. H. Shalaby, and Z. Kawasaki, "Performance analysis of both shot- and thermal-noise limited multipulse PPM receivers in gamma–gamma atmospheric channels," *J. Lightwave Technol.*, vol. 31, no. 19, pp. 3142–3150, Oct. 2013.

[15] N. Aoki, T. Ohtsuki, and I. Sasase, "Performance analysis of multi-pulse pulse position modulation using avalanche photodiode in optical intersatellite links," *IEICE Trans. Commun.*, vol. E79-B, pp. 52–56, 1996.

[16] F. Xiong, *Digital Modulation Techniques*, 2nd ed. Artech House, 2006.

[17] X. Zhu and J. M. Kahn, "Free-space optical communication through atmospheric turbulence channels," *IEEE Trans. Commun.*, vol. 50, no. 8, pp. 1293–1300, Aug. 2002.

[18] R. L. Al-Habash, M. A. Andrews, and L. C. Phillips, "Mathematical model for the irradiance probability density function of a laser beam propagating through turbulent media," *Opt. Eng.*, vol. 40, no. 8, pp. 1554–1562, Aug. 2001.

[19] H. Al-Raweshidy and S. Komaki, *Radio Over Fiber Technologies for Mobile Communications Networks*, 1st ed. Norwell, MA: Artech House, 2002.

[20] K.-P. Ho, *Phase-Modulated Optical Communication Systems*. New York: Springer, 2005.

[21] Wolfram Function Site, Sept. 2016. [Online]. Available: http://functions.wolfram.com/.

[22] J. G. Proakis, *Digital Communications*. New York: McGraw-Hill, 1983.